EFFECT OF GRAPHENE OXIDE ON THE THERMAL PROPERTIES OF BOVINE HIDE POWDERS

Lan Luo, Hao Zhang, Jie Liu*, Keyong Tang*

College of Materials Science and Engineering, Zhengzhou University, Henan Zhengzhou, 450001.

a) Corresponding author: liujie@zzu.edu.cn, kytangzzu@hotmail.com

b) other authors: xixiliyaxue@163.com, 1825604345@qq.com

Abstract. Graphene oxide (GO) is one of the most interesting two-dimensional nanomaterials in recent years. In order to explore its potential application in leather making process, a study on evaluating the effects of GO on the thermal stability and thermal decomposition kinetics of bovine hide powders (HP) was performed by thermogravimetry. The results revealed that GO-doped hide powders (GO-HP) exhibit better thermal stability than those of raw hide powders. The kinetic and mechanism of the decomposition process were analyzed by using an integrated procedure involving model-free methods and universal master-plots method. Three methods were employed to determine the apparent activation energy of the samples, including the Flynn-Wall-Ozawa (FWO), Modified Kissinger-Akahira-Sunose (MKAS), and Friedman methods. The activation energy values of HP and GO-HP samples were found to be 240.45 and 184.66 kJ/mol, respectively. Comparison of the experimental and theoretical master plots of various reaction mechanisms indicated that when the conversion values are below 0.5, the most probable decomposition mechanism for both HP and GO-HP is One-dimensional diffusion (D1). Above 0.5, the decomposition mechanisms of HP and GO-HP are most probably described by Random Nucleation and nuclei growth (A3) and Phase boundary controlled reaction (R3) models, respectively.

Keywords. Graphene oxide, hide powder, thermal kinetic, activation energy

1 Introduction

Collagen is the most abundant structural protein in hides and skins, which has a rod-like triple-helical structure. The multilevel hierarchical structure of collagen and the presence of crystallization zone help to stabilize collagen fiber. However, when heated to a certain temperature, the triple helix chain is transformed into a disordered structure and denaturation occurs. Generally, when raw hides and skins are heated to above their denaturation temperature, they will shrink and a reduction of the area of collagen materials can be observed. For leathers, several tens or more than one hundred degrees centigrade could also induce irreversible denaturation, although collagen fibers were crosslinked by tanning agents. Higher temperatures will further result in decomposition and pyrolysis of leather. Therefore, improving the thermal stability of leather has been an important purpose during leather production. To achieve this goal, one should preferably have in-depth understanding of the thermal degradation kinetics and mechanism before any attempts are made to enhance the thermal stability of leather. Kronick et al. studied the thermal deformation behaviour of bovine skin collagen, and proposed that raw skin contains two different types of collagen [1]. Sundar et al. studied the effect of copolymer dispersions on properties of leather, they found that thermal stability increased with the increase of ionic content of dispersion [2]. Olivares et al. studied the effect of sodium montmorillonite on the thermal stability on leather [3].

Graphene oxide (GO) can be obtained by oxidation of graphene using strong acid and has the similar structure to graphene, which contains a two-dimensional network structure. It differs from graphene in the surface which contains more oxygen-containing functional groups such as -OH, C=O, and -COOH. As a result, GO is highly amphiphilic and can soluble in water and organic solvents, but the presence of these functional groups will also destroy the large π bond on the surface, reducing the electron transporting ability [4]. Also due to the presence of these reactive polar

groups and adsorbed water molecules on the surface of the graphene oxide, the single layer graphene oxide is thicker than the single layer graphene.

The use of graphene oxide as reinforcing filler can bring about improvements in mechanics, electricity, and thermal stability for polymer composites. Many researchers have studied the effect of GO on different kinds of polymers. Mo et al. [5] modified graphene oxide with cetyltrimethylamine and then added it into polyacrylic acid, resulting in composites with better conductivity. Kai et al. [6] filled polycaprolactone (PCL) with graphene oxide and found that the thermal stability and mechanical properties of PCL were significantly improved. In this work, GO was incorporated into hide fibers in order to improve their thermal properties. The activation energies of thermal decomposition of the fibers were first evaluated using several model-free methods, and then the degradation mechanisms were further analyzed using the master-plots method.

2 Materials and Experiences

Hide powders (HP) used in this work was prepared in our laboratory using delimed bovine split hide as the raw materials. Graphene oxide dispersion (0.05mg/ml) was purchased from Jining Leadernano Tech. Co., Ltd., China. GO doped hide powders (GO-HP) were fabricated by immersing hide powders into GO dispersions under gently magnetic stirring for 24 h. After washing in distilled water for several times, the fibers were freeze-dried and conditioned in a desiccator over silica gel for 1 week before analysis.

Thermogravimetry tests were performed on a Mettler Toledo thermogravimetric instrument (TGA/ DSC 1), which allowable range of sample quality is 8-15mg. In each test, around 10 mg of GO-HP sample was spread uniformly on the bottom of the alumina crucible. The pyrolysis experiments were performed at heating rates of 5, 10, 20, and 30 °C/min in a dynamic high purity nitrogen flow of 40 ml/min. The temperature of the furnace was programmed to rise from room temperature to 600 °C.

2.1 Kinetic methods

ICTAC Kinetics Committee recommends the appropriate ways for calculating kinetic data and kinetic computations like apparent activation energy (E), pre-exponential factor (or the frequency factor, A) and mechanism function [7]. The single-step kinetic equation of solid sample at isothermal prerequisite is described as Eq. (1).

$$\frac{d\alpha}{dt} = k(T) f(\alpha) \tag{1}$$

Where α is the extent of conversion (Eq. (2)), and m_t, m_0, and m_f are the weight at time t, initial and final mass of the sample, respectively.

$$\alpha = \frac{m_t - m_0}{m_f - m_0} \tag{2}$$

The kinetic constant k can be expressed using the Arrhenius model, which is a function of the temperature with the universal gas constant R and activation energy E.

$$k = Ae^{-\frac{E}{RT}} \tag{3}$$

The kinetic parameters E and A can be determined by differential method. This involves introducing β, the linear heating rate:

$$\beta = \frac{dT}{dt} \tag{4}$$

Thus, substituting for Eq. (3) and (4) in Eq. (1) gives:

$$\beta\left(\frac{d\alpha}{dT}\right)=Af(\alpha)\exp\left(-\frac{E}{RT}\right) \tag{5}$$

which is the commonly used kinetic equation of the heterogeneous reaction.

It is known that the model-free isoconversional or non-isoconversional methods are very useful for estimating apparent activation energy regardless of the reaction mechanism. Three model-free methods were used in this study. Through each given α corresponding to temperatures of the weight loss data at four different heating rates, ln ($\beta/T^{1.92}$), ln(β) and ln(dα/dt) against 1/T can be straight lines and the apparent activation energy can be calculated from the slope.

$$\ln\left(\frac{\beta_i}{T_{\alpha,i}^{1.92}}\right)=Const-1.0008\left(\frac{E_\alpha}{RT_\alpha}\right) \tag{6}$$

$$\ln\beta_i=Const-1.052\left(\frac{E_\alpha}{RT_\alpha}\right) \tag{7}$$

$$\ln\left(\frac{d\alpha}{dt}\right)_\alpha=\ln\left[f(\alpha)A_\alpha\right]-\frac{E_\alpha}{RT_\alpha} \tag{8}$$

2.2 Generalized master plots method

The generalized time (θ), introduced by Ozawa, was used for the universal master plots and was valid for experimental data recorded under any heating profile [8], which was defined as:

$$\theta=\int_0^t e^{(-E/RT)}dt \tag{9}$$

Another form can be obtained by differentiating Eq. (9):

$$\frac{d\theta}{dt}=e^{(-E/RT)} \tag{10}$$

The substitution of Eq. (10) into Eq. (1) leads to:

$$\frac{d\alpha}{d\theta}=Af(\alpha) \tag{11}$$

α=0.5 was used as a reference point, then Eq. (11) becomes:

$$\frac{d\alpha/d\theta}{(d\alpha/d\theta)_{0.5}}=\frac{f(\alpha)}{f(0.5)} \tag{12}$$

Eq. (12) indicates that, for a given α, the expression $(d\alpha/d\theta)/(d\alpha/d\theta)_{\alpha=0.5}$ would be equivalent to f(α)/f (0.5). From Eq. (10) and (11), the relationship between the generalized reaction rate and the experimental data can be established:

$$\frac{d\alpha/d\theta}{(d\alpha/d\theta)_{0.5}}=\frac{d\alpha/dt}{(d\alpha/dt)_{0.5}}\frac{e^{(E/RT)}}{e^{(E/RT_{0.5})}} \tag{13}$$

where $T_{0.5}$ is the temperature corresponding to α=0.5. This function implied that the experimental mater plots need a predetermined activation energy value under non-isothermal conditions. Table 1 lists the most frequently used reaction models and functions, including the recently proposed random scission model [8].

Table 1. *f* (α) kinetic functions for the most frequently used reaction mechanisms of solid state processes.

Symbol	Reaction mechanism	$f(\alpha)$
A2	Random Nucleation and nuclei growth (Avrami-Erofeev, n=2)	$2(1-\alpha)[-\ln(1-\alpha)]^{1/2}$
A3	Random Nucleation and nuclei growth (Avrami-Erofeev, n=3)	$3(1-\alpha)[-\ln(1-\alpha)]^{2/3}$
A4	Random Nucleation and nuclei growth (Avrami-Erofeev, n=4)	$4(1-\alpha)[-\ln(1-\alpha)]^{3/4}$
An	Random Nucleation and nuclei growth	$n(1-\alpha)[-\ln(1-\alpha)]^{(n-1)/n}$
D1	One-dimensional diffusion	0.5α
D2	Two-dimensional diffusion (Valensi)	$[-\ln(1-\alpha)]^{-1}$
D3	Three-dimensional diffusion (Jander)	$3(1-\alpha)^{2/3}/2[1-(1-\alpha)^{1/3}]$
D4	Three-dimensional diffusion (Ginstling - Brounstein)	$(3/2)[1-(1-\alpha)^{1/3}]^{-1}$
F1	First-order reaction	$1-\alpha$
F2	Second-order reaction	$(1-\alpha)^2$
F3	Third-order reaction	$(1-\alpha)^3$
R2	Phase boundary controlled reaction (contracting area)	$2(1-\alpha)^{1/2}$
R3	Phase boundary controlled reaction (contracting volume)	$3(1-\alpha)^{2/3}$
L2	Random scission	$2(\alpha^{1/2}-\alpha)$

3 Results

The thermogravimetric experiments were carried out at four different heating rates (5, 10, 20 and 30 °C/min) at an inert atmosphere of nitrogen. The continuous shift of TG and DTG curves to higher temperatures can be observed with the increase in heating rate. This is typical for all nonisothermal experiments within a range of heating rate due to the existence of temperature gradient throughout the cross-section of the samples. From Fig. 1 and Fig. 2, the thermal decomposition process of both HP and GO-HP can be divided into three stages of weight loss for a heating rate of 10°C min^{-1} in the temperature range from room temperature to 600 °C. The first stage goes from room temperature to around 150°C. There are many hydrophilic groups on collagen molecules, which will inevitably absorb a certain amount of water during storage. This weight loss stage is most likely due to the evaporation of water absorbed from the fibers. The second stage, from 150 to 550°C, showing the obvious weight loss corresponding to the main composition of the collagen fibers. A high DTG peak can be found at around 330°C. A small shoulder peak appeared on DTG curves of HP at about 230°C. A more prominent shoulder peak can be observed at about 200°C on DTG curve of GO-HP. This could be attributed to the degradation of free GO, as reported by Song et al. [9] and Guo et al. [10]. The third stage, from 550 to 600°C, is the slow decomposition of carbonaceous matters accounting for less than 5% of the total mass loss.

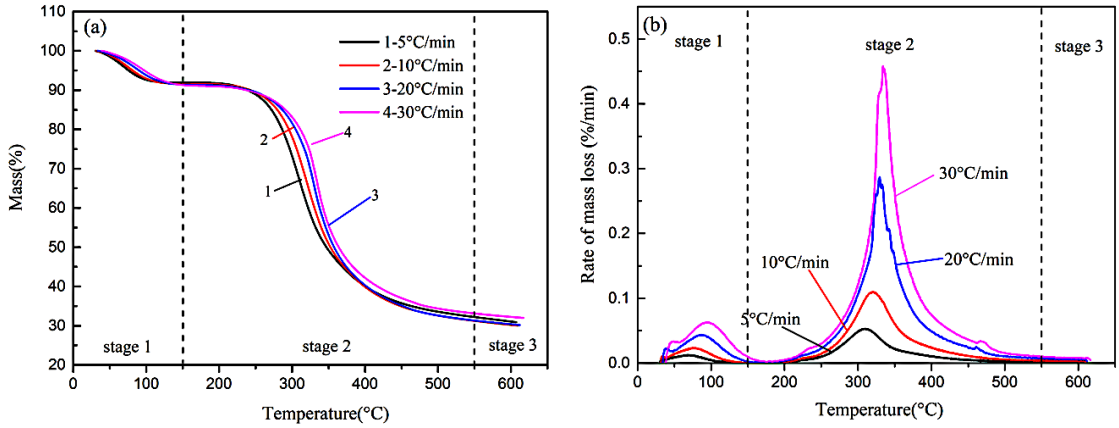

Fig. 1. (a) TG and (b) DTG curves of HP at heating rates of 5, 10, 20, 30°C /min.

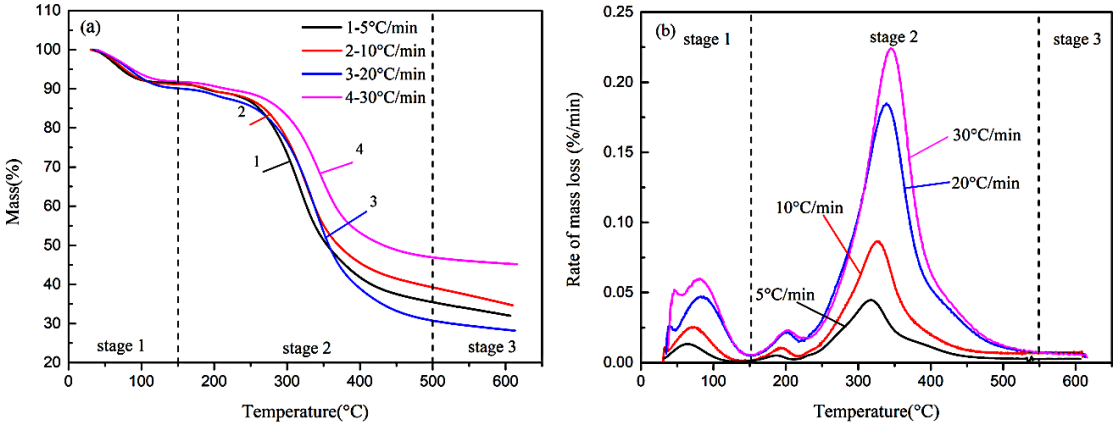

Fig. 2. (a) TG and (b) DTG curves of GO-HP at heating rates of 5, 10, 20, 30°C /min.

Fig. 3 shows a comparison of the TG and DTG curves of HP and GO-HP at a heating rate of 10°C/min. In order to further evaluate the effect of GO on thermal stability of hide fibers, we considered the temperature of the maximum rate of degradation as the decomposition temperature (T_{max}), onset temperature of decomposition (T_{onset}), the temperature of the degradation process at which 50% weight loss occurs ($T_{50\%}$) and the solid residues remaining at 600°C (Table 2). It can be found that the T_{onset} and T_{max}, which are considered as indicators for structural destabilization of polymers, increased after the incorporation of GO into the hide fibers. The $T_{50\%}$ value of GO-HP is higher than that of the HP, suggesting that GO can delay the degradation of hide fibers and improve the thermal stability in the initial stage of thermal decomposition. The improvement of thermal stability of hide fiber is more likely related to the strengthening effect of GO, which can restrict the molecular mobility of the macromolecular (collagen) chains in the solid state.

Table 2. The temperature corresponding to the onset temperature of the main degradation (T_{onset}), maximum rate of mass loss (T_{max}), the temperature corresponding to 50% mass loss ($T_{50\%}$) and the residue at 600°C at a heating rate of 10°C min^{-1}.

Samples	T_{onset}(°C)	T_{max}(°C)	$T_{50\%}$(°C)	Residues remaining at 600°C (%)
HP	279.17	322.89	353.46	30.13
GO-HP	283.45	326.89	372.51	35.04

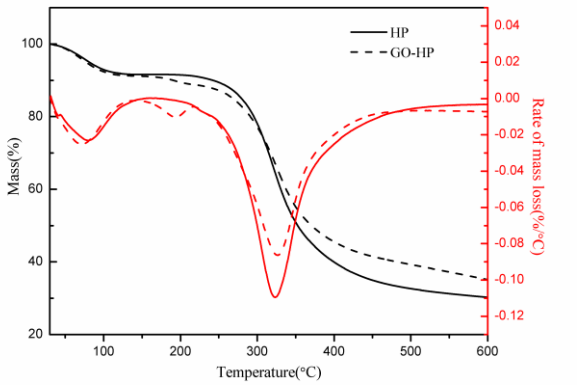

Fig. 3. TG and DTG curves of HP and GO-HP at a heating rate of 10°C /min.

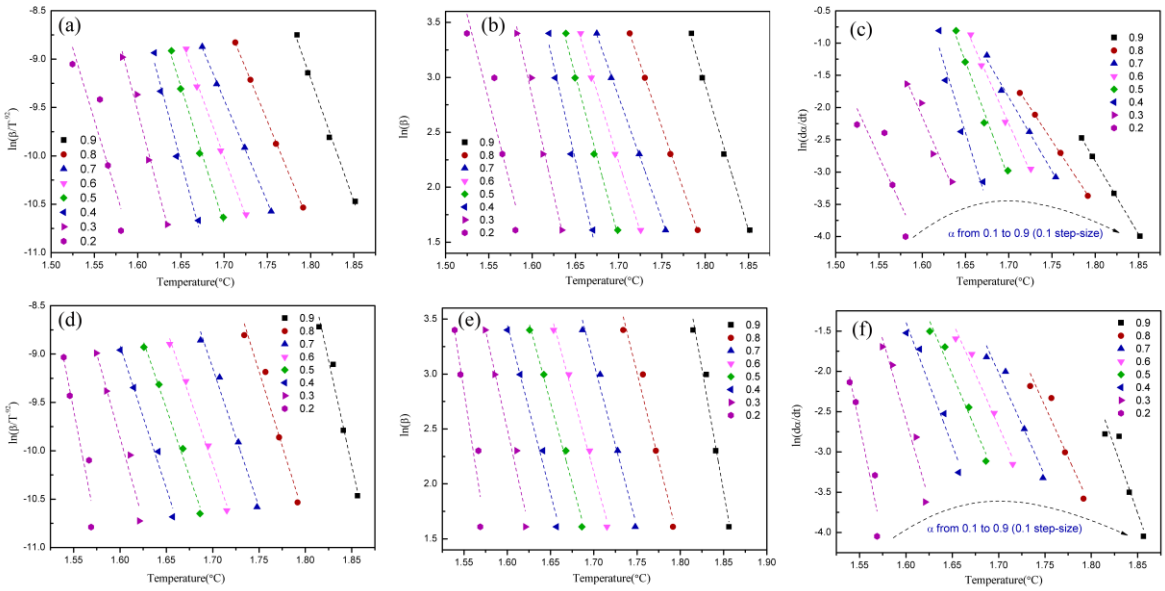

Fig. 4. Typical iso-conversional plots of (a,d) MKAS, (b,e) FWO and (c,f) Friedman methods of (a,b,c) HP and (d,e,f) GO-HP.

Activation energy is considered as a measurement of the energy barrier to a controlling (rate limiting) bond rupture or bond redistribution step. According to the plots of $\ln(\beta/T^{1.92})$, $\ln(\beta)$, and $\ln(d\alpha/dt)$ against 1/T (Fig. 4), the linear fitting can be straight lines, and the activation energy values can be obtained from the slopes. The E results of HP and GO-HP obtained by MKAS, FWO and Friedman methods are shown in Table 3. The results calculated based on MKAS method was chosen in the following mechanism analysis, according to the suggestion of Criado et al. [11]. The average thermal degradation activation energy of HP is calculated to be 226.88 kJ/mol, and that of GO-HP is 283.30 kJ/mol. It can be concluded that the incorporation of GO into hide fibers increases the activation energy of thermal degradation of HP by around 25%. From the activation energy results as well as other thermal degradation parameters, it can be concluded that the graphene oxide can enhance the thermal stability of raw hide materials. That may be due to that a large amount of graphene oxide adsorbs on the surface of collagen, forming a protective shell-like structure, which protects collagen from thermal degradation during the heating process.

Table 3 Activation energy (E) results of HP and GO-HP based on MKAS, FWO and Friedman methods.

α	HP (kJ/mol)			GO-HP (kJ/mol)		
	MKAS	FWO	Friedman	MKAS	FWO	Friedman
0.2	247.02	244.77	244.81	412.00	401.70	470.46
0.3	285.45	280.98	257.35	287.40	282.90	331.67
0.4	276.42	272.18	360.32	245.22	242.60	254.12
0.5	236.43	234.01	301.04	233.47	231.27	225.51
0.6	202.42	201.54	248.34	232.38	230.07	216.57
0.7	175.83	176.12	190.97	238.44	235.67	212.91
0.8	180.79	180.65	169.05	256.39	252.52	210.99
0.9	210.65	208.74	187.97	361.08	351.77	271.21
Average	226.88	224.87	244.98	283.30	278.56	274.18

Fig.5 shows the theoretical generalized master plots corresponding to the kinetic models calculated by f(α)/f(0.5) using the expressions in Table 1, and the experimental results obtained at different heating rates. When the conversion is less than 0.5, the model of both HP and GO-HP is close to the D1, indicating that the degradation mechanism of them refers to one-dimensional diffusion model. However, when α>0.5, degradation of HP is most probably regulated by random nucleation and nuclei growth (A3), and GO-HP changed the kinetic model to phase boundary controlled reaction (R2). Liang et al. [12] reported a similar degradation model of graphene nano-platelets composite materials. The results of the present study provide useful information for fabricating high-performance leather.

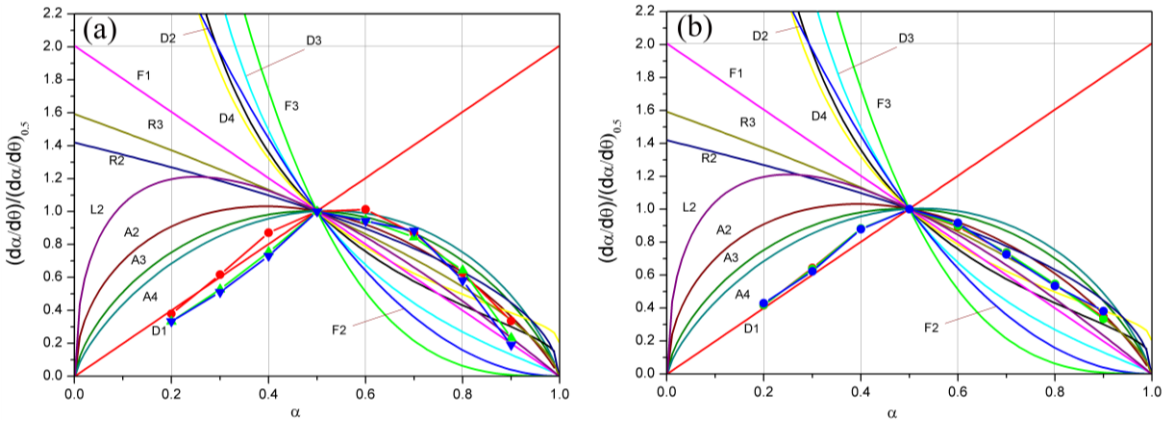

Fig. 5. Master curves and experimental data obtained for (a) HP and (b) GO-HP at different heating rates.

4 Conclusions

The thermal degradation process of the HP and GO-HP can be divided into three stages: water loss stage, thermal degradation stage and slow decomposition stage. The obtained GO-HP sample shows an enhancement in the thermal properties in the temperature range from room temperature to 600 °C. The isoconversional kinetic study of the thermal decomposition was performed using Flynn-Wall-Ozawa (FWO), Modified Kissinger-Akahira-Sunose (MKAS), and Friedman methods. The

most probable mechanism of thermal decomposition was suggested by comparison between experimental and theoretical master plots. The reaction model for both both HP and GO-HP is D1 when the α is less than 0.5. When α>0.5, the degradation models for HP and GO-HP are corresponding to A3 and R2, respectively.

References

1. *Paul Kronick, Beverly Maleeff & Robert Carroll.: 'The Locations of Collagens with Different Thermal Stabilities in Fibrils of Bovine Reticular Dermis', Connect. Tissue Res., 18,123-134, 2009.*
2. *Steffen Maier, Alexander Sunder, Holger Frey et al.: 'Synthesis of poly (glycerol) - block - poly(methyl acrylate) multi-arm star polymers', Polymer Crystallization, 21, 226-230, 2000.*
3. *G.Sanchez-Olivares, A.Sanchez-Solis, F.Calderasb, et al.: 'Sodium montmorillonite effect on the morphology, thermal, flame retardant and mechanical properties of semi-finished leather', Appl. Clay Sci., 102, 254-260, 2014.*
4. *P. Budrugeac, Andrei Cucos, Lucreţia Miu.: 'The use of thermal analysis methods for authentication and conservation state determination of historical and/or cultural objects manufactured from leather', J. Therm. Anal. Calorim., 104, 438-450, 2011.*
5. *Jinpeng Mo, Wenshi Ma, Guorong Qiu et al.: 'Mesoporous silica coated graphene oxide: fabrication, characterization and effects on the dielectric properties of its organosilicon hybrid films', J. Mater. Sci. - Mater. Electron., 30, 130-146, 2019.*
6. *Weihua Kai, Yuuki Hirota, Lei Hua et al.: 'Thermal and mechanical properties of a poly (ϵ-caprolactone)/graphite oxide composite', J. Appl. Polym. Sci., 107, 1395-1400, 2008.*
7. *Sergey Vyazovkin, Alan K.Burnham, José M.Criado et al.: 'ICTAC Kinetics Committee recommendations for performing kinetic computations on thermal analysis data', Thermochim. Acta, 520, 1-19, 2011.*
8. *Starink MJ.: 'The determination of activation energy from linear heating rate experiments: a comparison of the accuracy of isoconversion methods', Thermochim. Acta, 404, 163-176, 2003.*
9. *Pingan Song, Zhenhu Cao, Yuanzheng Cai, et al.: 'Fabrication of exfoliated graphene-based polypropylene nanocomposites with enhanced mechanical and thermal properties', Polymer, 52, 4001-4010, 2011.*
10. *Sheng Guo, Gaoke Zhang, Yadan Guo, et al.: 'Graphene oxide–Fe2O3 hybrid material as highly efficient heterogeneous catalyst for degradation of organic contaminants', Carbon, 60, 437-444, 2013.*
11. *Criado JM, Pérez-Maqueda LA, Gotor FJ, et al.: 'A unified theory for the kinetic analysis of solid state reactions under any thermal pathway', J. Therm. Anal. Calorim., 72, 901-906, 2003.*
12. *J.Z.Liang, J.Z.Wang, Gary C.P et al.: 'Thermal decomposition kinetics of polypropylene composites filled with graphene nanoplatelets', Polym. Test., 48, 97-103, 2015.*